JLAB-THY-99-04

STRANGENESS IN THE NUCLEON
or
the quark model beyond the valence approximation

Nathan Isgur
Jefferson Lab
12000 Jefferson Avenue, Newport News, Virginia 23606

Simple arguments based on unitarity indicate that meson loops diagrams, induced by an underlying $q\bar{q}$ pair creation process, should badly disturb the phenomenologically successful spectrscopy and dynamics of the valence quark model, including such simple but mysterious regularities as the OZI rule. I will discuss some recent progress in adding pair creation to the valence quark model in a way which provides a rationale for the quark model's success.

1 Introductory Remarks

QCD is undeniably very complex, so if we are to understand it, we will clearly have to find some way to simplify it. In particular, I believe that the central issue in strong QCD [1] is to identify the correct low energy degrees of freedom at the "quark model" scale $\mu_{QM} \sim 1$ GeV. Hadronic physics of course shares the analog of this critical problem with most other parts of physics where, even though the basic interaction might be known, the phenomena of interest involve complex systems.

In these lectures I will argue that there are many good reasons to believe that the valence quark model is a good starting point in this quest. First of all, when extended *via* the flux tube model, wherein the gluonic degrees of freedom are subsumed into flux tubes, the constituent quark model can be mapped onto QCD in the large N_c limit [2]. After reviewing these matters, I will argue that, while adequate for many purposes, this quark model must be further extended by the addition of pair creation (a $1/N_c$ effect) if it is to provide a satisfactory qualitative picture of low energy strong interaction dynamics. That is, I suggest that dynamical $q\bar{q}$ pairs are the key missing ingredient of the constituent quark model. In particular, I will show in an explicit model how one can "unquench" the quark model without spoiling its spectroscopic successes or ruining the OZI rule[3]. At the same time, I will show that while each light quark flavor may make a relatively small contribution to the net proton spin of order $1/N_c$, N_f such contributions can account for the observed "spin crisis".

2 Proposal for a general Framework

As already mentioned, I believe that the key to a qualitative understanding of strong QCD is the same as in most other areas of physics: identifying the appropriate degrees of freedom. For example, atomic physics is based on taking the nuclei and electrons as the low energy effective degrees of freedom, with the underlying effects of nucleons subsumed into static nuclear properties and those of photons into low energy effective potentials; nuclear physics is in turn very well-described by nucleons moving in an empirical nucleon-nucleon potential.

Foremost among the puzzles we face in strong QCD is in fact a glaring "degree of freedom" problem: the established low energy spectrum of QCD behaves as though it is built from the degrees of freedom of spin-$\frac{1}{2}$ fermions confined to a $q\bar{q}$ or qqq system. Thus, for mesons we seem to observe a "quarkonium" spectrum, while for the baryons we seem to observe the spectrum of the two relative coordinates of three spin-$\frac{1}{2}$ degrees of freedom.

These apparent degrees of freedom are to be contrasted with the most naïve interpretation of QCD which would lead us to expect a low energy spectrum exhibiting 36 quark and antiquark degrees of freedom (3 flavors $\times$ 2 spins $\times$ 3 colors for particle and antiparticle), *and* 16 gluon degrees of freedom (2 spins $\times$ 8 colors). Less naïve pictures exist, but none evade the puzzle of the missing gluonic degrees of freedom in the low energy spectrum.

The second major "degree of freedom problem", and the one on which I will focus here, has to do with $q\bar{q}$ pair creation. At least naïvely, one would expect pair creation to be so strong that a valence quark model would fail dramatically. That pair creation should be expected to lead to dramatic failures of valence quark model spectroscopy and dynamics is true even though we know empirically (and theoretically) that pair creation is suppressed, *i.e.*, that the observed hadronic spectrum is dominated by relatively narrow resonances. More specifically, there are three main puzzles associated with the nature and importance of such $q\bar{q}$ pairs in low energy hadron structure:

1. the origin of the apparent valence structure of hadrons (since even in the large N_c limit to be described in the next section, "Z-graphs" would produce pairs unless the quarks were heavy),

2. the apparent absence of unitarity corrections to naïve quark model spectroscopy, despite one's expectation of mass shifts $\Delta m \sim \Gamma$ (where Γ is a typical hadronic width), and

3. the systematic suppression of OZI-violating amplitudes A_{OZI}, relative to one's expectation (from unitarity) that $A_{OZI} \sim \Gamma$.

Before addressing these problems associated with $q\bar{q}$ pairs, I first briefly review the general framework in which I believe we must view the valence quark model. This framework is based on results from three different directions which converge on a simple picture of the structure of strong QCD: valence plus glue dominance with $q\bar{q}$ corrections.

2.1 The Large N_c Limit of QCD

It is now widely appreciated that many of the observed features of the strong interactions can be rationalized in QCD within the $1/N_c$ expansion [2]. Moreover, there is growing evidence from lattice QCD that while $N_c = 3$ might not be sufficiently large for the $1/N_c$ expansion to be used quantitatively, the main qualitative features of QCD (including confinement and the spontaneous breakdown of chiral symmetry) are independent of N_c.

We should therefore take seriously the fact that it can be shown in the large-N_c limit that hadron two-point functions are dominated by graphs in which the valence quark lines propagate from their point of creation to their point of annihilation without additional quark loops. A form of the OZI rule [3] also emerges naturally. Large-N_c QCD thus presents a picture of narrow resonances interacting weakly with hadronic continua. In this picture the resonances themselves are made of valence quarks and glue.

2.2 Quenched QCD

Quenched lattice QCD provides other new insights into QCD. In quenched QCD the lattice sums amplitudes over all time histories in which no $q\bar{q}$ loops are present. It thus gives quantitative results from an approximation with many elements in common with the large N_c limit. One of the most remarkable features of these calculations is that despite what would seem to be a drastic approximation, they provide a reasonably good description of low energy phenomenology. Indeed, for various intermediate quantities like the QCD string tension they provide very good approximations to full QCD results with the true lattice coupling constant replaced by an effective one. In quenched QCD, as in the large N_c limit, two point functions thus seem to be well-approximated by their valence content (namely pure glue for glueballs, $q\bar{q}$ plus glue for mesons, and qqq plus glue for baryons).

In comparing the large N_c limit and quenched lattice QCD we note that:

- In both pictures all resonances have only valence quarks, but they have an unlimited number of gluons. Thus they support valence models for mesons and baryons, but not for glueballs or for the gluonic content of mesons and baryons.

- In both pictures a propagating valence quark has contributions from not only a positive energy quark propagator, but also from "Z-graphs". (A "Z-graph" is a time-ordered graph in which the interactions first produce a pair and then annihilate the antiparticle of the produced pair against the original propagating particle). Cutting through a two-point function at a fixed time therefore would in general reveal not only the valence quarks but also a large $q\bar{q}$ sea. This does not seem to correspond to the usual valence approximation. Consider, however, the Dirac equation for a single light quark interacting with a static color source (or a single light quark confined in a bag). This equation represents the sum of a set of Feynman graphs which also include Z-graphs, but the effects of those graphs is captured in the lower components of the single particle Dirac spinor. *I.e.*, such Z-graphs correspond to relativistic corrections to the quark model. That such corrections are important in the quark model has been known for a long time. For us the important point is that while they have quantitative effects on quark model predictions (*e.g.*, they are commonly held to be responsible for much of the required reduction of the nonrelativistic quark model prediction that $g_A = 5/3$ in neutron beta decay), they do not qualitatively change the single-particle nature of the spectrum of the quark of our example, nor would they qualitatively change the spectrum of $q\bar{q}$ or qqq systems.

- Finally, we note that the large N_c and quenched approximations are *not* identical. For example, the NN interaction is a $1/N_c$ effect, but it is not apparently suppressed in the quenched approximation.

2.3 The Heavy Quark Limit

The third perspective from which there is support for the same picture is the heavy quark limit [4]. While this limit has the weakest theoretical connections to the light quark world, it has powerful phenomenological connections: see Fig. 1. We see from this picture that in mesons containing a single heavy quark, $\Delta E_{orbital}$ (the gap between, for example, the $J^{PC} = 1^{--}$ and 2^{++} states), is approximately independent of m_Q, as predicted in the heavy quark limit, while $\Delta E_{hyperfine}$ varies like m_Q^{-1} as expected.

Recall that in the heavy quark limit a hadronic two-point function is dominated by a single valence Q plus its associated "brown muck", with neither $Q\bar{Q}$ loops nor Q Z-graphs. The fact that heavy-quark-like behaviour persists all the

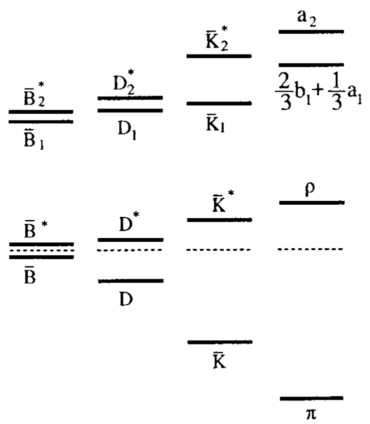

Figure 1: The $Q\bar{q}$ meson spectra as a function of the "heavy" quark mass.

way down to light quark masses suggests that light quarks, like heavy quarks, behave like single valence quarks and thus by extension that the "brown muck" behaves like a single valence antiquark.

Fig. 2 shows that heavy quark behaviour also apparently persists in a stronger form: the light meson spectrum appears to mimic the $Q\bar{Q}$ quarkonium spectrum. This is surprising since this latter spectrum depends on the decoupling of gluonic excitations (as opposed to glue) from the spectrum *via* an adiabatic approximation.

In view of this surprise, let us examine the nature of the adiabatic approximation in QCD. Consider first QCD without dynamical quarks in the presence of fixed $Q_1\bar{Q}_2$ or $Q_1Q_2Q_3$ sources[5,6]. The ground state of QCD with these sources in place will be modified, as will be its excitation spectrum. For excitation energies below those required to produce a glueball, this spectrum will presumably be discrete for each value of the $Q_1\bar{Q}_2$ relative spatial separation $\vec{r}$, with each eigenvalue being a continuous function of $|\vec{r}|$, as shown schematically in Fig. 3. There will be analogous spectra for $Q_1Q_2Q_3$ which are functions of its two relative coordinates. We call the energy surface traced out by a given level of excitation as the positions of the sources are varied an adiabatic surface, and *define* the "quark model limit" to be applicable when the quark sources move along the lowest adiabatic surface.

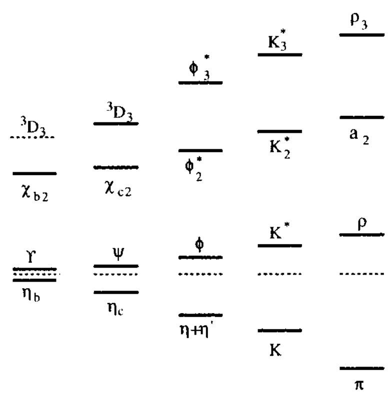

Figure 2: The $Q\bar{Q}$ meson spectra as a function of the "heavy" quark mass.

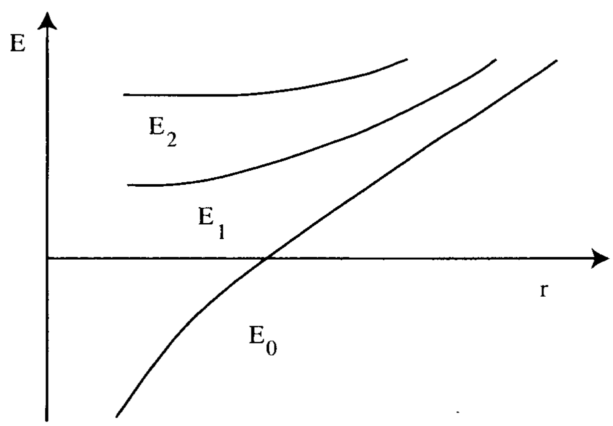

Figure 3: Schematic of the low-lying adiabatic surfaces of $Q_1\bar{Q}_2$ at separation r; $E_0(r)$ is the gluonic ground state, $E_1(r)$ the first excited state, *etc.*.

We all know a simple molecular physics analogy to this approximation. Diatomic molecular spectra can be described in an adiabatic approximation by holding the two relevant atomic nuclei at fixed separation r and then solving the Schrödinger problem for the (mutually interacting) electrons moving in the static electric field of the nuclei. The electrons will, for fixed r, have a ground state and excited states which will eventually become a continuum above energies required to ionize the molecule. The resulting adiabatic energy functions (when added to the internuclear Coulomb energy) then serve as effective internuclear potentials on which vibration-rotation spectra can be built. Molecular transitions can then take place within states built on a given surface or between surfaces.

In the "quark model limit" the quark sources play the rôle of the nuclei, and the glue plays the rôle of the electrons. From this point of view we can see clearly that conventional meson and baryon spectroscopy has only scratched the surface of even $q_1\bar{q}_2$ and $q_1q_2q_3$ spectroscopy: so far we have only studied the vibration-rotation bands built on the lowest adiabatic surface corresponding to the gluonic ground state. We should expect to be able to build other "hadronic worlds" on the surfaces associated with excited gluonic states [5].

While the adiabatic approximation is more general, it is becoming increasingly firmly established that this approximation is realized in QCD in terms of the development of a confining chromoelectric flux tube. These flux tubes are the analog of the Abrikosov vortex lines that can develop in a superconductor subjected to a magnetic field, with the vacuum acting as a dual (*i.e.*, electric) superconductor creating a chromoelectric Meissner effect. A $Q\bar{Q}$ system held at fixed separation $r >> \Lambda_{QCD}$ is known to have as its ground state a flux tube which leads to an effective low energy (adiabatic) potential corresponding to the standard "quarkonium" potential. However, this system also has excited states, corresponding to gluonic adiabatic surfaces in which a phonon has been excited in the flux tube, and on which spectra of "hybrid states" are built.

Lattice results allow us to check many aspects of the flux tube picture. For example, the lattice confirms the flux tube model prediction that sources with triality are confined with a string tension proportional to the square of their color Casimir. The predicted strongly collimated chromoelectric flux lines have also been seen on the lattice. I have found it particularly encouraging that the first excited adiabatic surfaces have been seen [7] with an energy gap $\delta V(r) = \pi/r$ above the quarkonium potential as predicted [5], and with the expected doubly-degenerate phonon quantum numbers (see Fig. 4). This strongly suggests that the J^{PC} exotic hybrid mesons predicted ten years ago [5] exist.

The flux tube model thus offers a possible explanation for one of the most puzzling apparent inconsistencies between the naïve quark model and QCD.

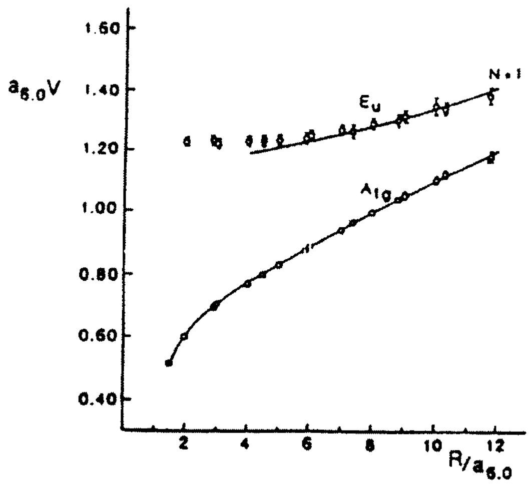

Figure 4: The ground state and first excited adiabatic potentials from lattice QCD [7].

Moreover, as discussed above, in the large N_c limit of QCD hadrons do indeed consist of just their valence quarks and the glue between them. Thus the flux tube model may legitimately be viewed as a candidate realization of QCD in the large N_c limit which is in addition consistent with insights into strong QCD which have emerged from quenched lattice QCD and from heavy quark theory.

3 Unquenching the Quark Model

The valence quark plus glue dominance embodied in the flux tube model can at best be a starting point for a systematic description of strong QCD, since we know that $q\bar{q}$ pair creation plays an important rôle in many phenomena. Nevertheless, näively attempting to add $q\bar{q}$ pair creation to the valence quark model leads to a number of very serious problems. These problems, which were mentioned briefly in Section 2, and potential solutions to them have been extensively discussed in a series of papers on "unquenching" the quark model [8,9,10]. In the following I briefly describe these solutions.

3.1 The Origin and Resiliency of Potential Models

In the preceeding Section, we saw that one of the "degrees of freedom" problems of the valence quark model could plausibly be solved by the flux tube model: the apparent absence of low energy degrees of freedom associated with the glue. The second "degree of freedom" problem is the apparent absence of excitations associated with the strong $q\bar{q}$ sea. Very closely related to this puzzle is the apparent unimportance of strong meson loop corrections.

A simple resolution of this puzzle has been proposed which is an extenion of the adiabatic approximation to the flux tube: the *full* quark potential model arises from an adiabatic approximation *including* the extra $q\bar{q}$ degrees of freedom embodied in the flux tube. At short distances where perturbation theory applies, the effect of N_f types of light $q\bar{q}$ pairs is (in lowest order) to shift the coefficient of the Coulombic potential from $\alpha_s^{(0)}(Q^2) = \frac{12\pi}{33 ln(Q^2/\Lambda_0^2)}$ to $\alpha_s^{(N_f)}(Q^2) = \frac{12\pi}{(33-2N_f) ln(Q^2/\Lambda_{N_f}^2)}$. The net effect of such pairs is thus to produce a *new* effective short distance $Q\bar{Q}$ potential. Similarly, when pairs bubble up in the flux tube (*i.e.*, when the flux tube breaks to create a $Q\bar{q}$ plus $q\bar{Q}$ system and then "heals" back to $Q\bar{Q}$), their net effect is to cause a shift $\Delta E_{N_f}(r)$ in the ground state gluonic energy which in turn produces a new long-range effective $Q\bar{Q}$ potential.

It has indeed been shown [8] that the net long-distance effect of the bubbles is to create a new string tension b_{N_f} (*i.e.*, that the potential remains linear). Since this string tension is to be associated with the observed string tension, after renormalization *pair creation has no effect on the long-distance structure of the quark model in the adiabatic approximation.* Thus the net effect of mass shifts from pair creation is much smaller than one would naïvely expect from the typical width Γ: shifts that are not absorbed into the physical string tension can only arise from nonadiabatic effects. For heavy quarkonium, these shifts can in turn be associated with states which are strongly coupled to nearby thresholds [11].

It should be emphasized that no simple truncation of the set of all meson loop graphs can reproduce such results: to recover the adiabatic approximation requires summing over large towers of $Q\bar{q}$ plus $q\bar{Q}$ intermediate states to allow a duality with the $q\bar{q}$ loop diagrams which have strength at high energy.

3.2 The Survival of the OZI Rule

There is another puzzle of hadronic dynamics which is reminiscent of this one: the success of the OZI rule [3]. A generic OZI-violating amplitude A_{OZI} can also be shown to vanish like $1/N_c$. However, there are several unsatisfactory features of this "solution" to the OZI mixing problem [12]. Consider ω-ϕ mixing as an example. This mixing receives a contribution from the virtual hadronic loop process $\omega \rightarrow K\bar{K} \rightarrow \phi$, both steps of which are OZI-allowed, and each of which scales with N_c like $\Gamma^{1/2} \sim N_c^{-1/2}$. The large N_c result that this OZI-violating amplitude behaves like N_c^{-1} is thus not peculiar to large N_c: it just arises from "unitarity" in the sense that the real and imaginary parts of a generic hadronic loop diagram will have the same dependence on N_c. The usual interpretation of the OZI rule in this case - - - that "double hairpin graphs" are dramatically suppressed - - - is untenable in the light of these OZI-allowed loop diagrams, which expose the deficiency of the large N_c argument: $A_{OZI} \sim \Gamma$ is *not* a good representation of the OZI rule. (Continuing to use ω-ϕ mixing as an example, we note that $m_\omega - m_\phi$ is numerically comparable to a typical hadronic width, so the large N_c result would predict an ω-ϕ mixing angle of order unity in contrast to the observed pattern of very weak mixing which implies that $A_{OZI} << \Gamma << m$.)

Unquenching the quark model thus endangers the naïve quark model's agreement with the OZI rule. It has been shown [9] how this disaster is naturally averted in the flux tube model through a "miraculous" set of cancellations between mesonic loop diagrams consisting of apparently unrelated sets of mesons (*e.g.*, the $K\bar{K}$, $K\bar{K}^* + K^*\bar{K}$, and $K^*\bar{K}^*$ loops tend to strongly cancel against loops containing a K or K^* plus one of the four strange mesons of the $L = 1$ meson nonets). Of course the "miracle" occurs for a good reason: the sum of *all* hadronic loops is dual to two $q\bar{q}$ hairpins of different flavors created and destroyed by a $^3P_0$ operator [13,14,15], but in the closure approximation such an operator cannot create mixing in other than a scalar channel.

While slightly more complex, it should be noted that OZI-violating baryon couplings like $p \rightarrow p\phi$ can be induced by loop diagrams which are essentially identical to those responsible for $\omega - \phi$ mixing. The same mechansism which prevents $\omega - \phi$ mixing also prevents such OZI-violating couplings.

3.3 Some Comments

The preceding discussion indicates that models which have not addressed the effects of unquenching on spectroscopy and the OZI rule should be viewed very skeptically as models of the effects of the $q\bar{q}$ sea on hadron structure: large towers of mesonic loops are required to understand how quarkonium spectroscopy and the OZI rule survive once strong pair creation is turned on. In particular, while pion and kaon loops (which tend to break the closure approximation due to their exceptional masses) have a special role to play, they cannot be expected to provide a reliable guide to the physics of $q\bar{q}$ pairs.

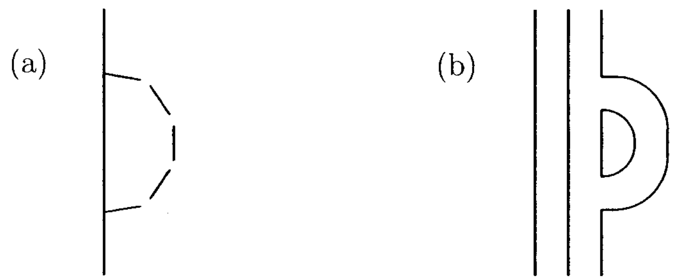

Figure 5: A meson loop correction to a baryon propagator, drawn at (a) the hadronic level, and (b) the quark level.

4 A Pair Creation Model for the Strangeness of the Proton

The strangeness content of the proton arises from the quark-level process shown in Fig. 5. The main new feature of the calculation on which this discussion is based [10] is a sum over a *complete set* of strange intermediate states, rather than just a few low-lying states. As explained above, this is *necessary* for consistency with the OZI rule and the success of quark model spectroscopy.

The lower vertex in Fig. 5 arises when $s\bar{s}$ pair creation perturbs the initial nucleon state vector so that, to leading order in pair creation,

$$|p\rangle \to |p\rangle + \sum_{Y^*K^*\ell S} \int q^2 dq \; |Y^*K^*q\ell S\rangle \, \frac{\langle Y^*K^*q\ell S\, |h_{s\bar{s}}|\, p\rangle}{M_p - E_{Y^*} - E_{K^*}} \,, \tag{1}$$

where $h_{s\bar{s}}$ is the $s\bar{s}$ quark pair creation operator, Y^* (K^*) is the intermediate baryon (meson), q and ℓ are the relative radial momentum and orbital angular momentum of Y^* and K^*, and S is the sum of their spins. This process will generate non-zero expectation values for strangeness observables:

$$\begin{aligned} \langle O_s\rangle \;&=\; \sum_{\substack{Y^*K^*\ell S \\ Y^{*\prime}K^{*\prime}\ell' S'}} \int q^2dq\, q'^2dq' \, \frac{\left\langle p\, |h_{s\bar{s}}|\, Y^{*'}K^{*'}q'\ell' S'\right\rangle}{M_p - E_{Y^{*\prime}} - E_{K^{*\prime}}} \\ &\quad \times \left\langle Y^{*'}K^{*'}q'\ell' S'\, |O_s|\, Y^*K^*q\ell S\right\rangle \frac{\langle Y^*K^*q\ell S\, |h_{s\bar{s}}|\, p\rangle}{M_p - E_{Y^*} - E_{K^*}}. \end{aligned} \tag{2}$$

The derivation of this simple equation, including the demonstration that it is gauge invariant, is straightforward [10]. We will be considering the cases $O_s = \Delta s$, R_s^2, and μ_s, where Δs is the spin carried by the strange quark sea of the proton, and where R_s^2 and and μ_s are the proton's strangeness radius and magnetic moment.

To calculate the $p \to Y^* K^*$ vertices in Eq. (1), the flux-tube-breaking model was used. This model, which reduces to the well-known $^3P_0$ decay model in a well-defined limit, had its origin in applications to decays of mesons [13,14] and baryons [15]. The model assumes that a meson or baryon decays when a chromoelectric flux tube breaks, creating a constituent quark and antiquark on the newly exposed flux tube ends. The pair creation operator is taken to have $^3P_0$ quantum numbers:

$$h_{q\bar{q}}(t,\mathbf{x}) = \gamma_0 \left(\frac{3}{8\pi r_q^2}\right)^{3/2} \int d^3z \, \exp\left(-\frac{3z^2}{8r_q^2}\right) q^\dagger(t,\mathbf{x}+\frac{\mathbf{z}}{2})\alpha \cdot \nabla q(t,\mathbf{x}-\frac{\mathbf{z}}{2}) \,. \tag{3}$$

The dimensionless constant γ_0 is the intrinsic pair creation strength, a parameter which was fit to the $\Delta \to N\pi$ width. The operator (3) creates *constituent* quarks, hence the pair creation point is smeared out by a gaussian factor whose width, r_q, is another parameter of the model. The parameter r_q is constrained by meson decay data to be approximately 0.25 fm [8,9].

Once an $s\bar{s}$ pair is created, the decay proceeds by quark rearrangement, as shown in Fig. 6. Even with simple harmonic oscillator (SHO) wavefunctions, the sum over intermediate states would be very difficult were it not for an important selection rule: inspection of the quark line diagrams in Fig. 6 shows that the relative coordinate of the non-strange quarks in baryon Y^* is always in its ground state. Only the relative coordinate between the strange and non-strange quarks (*i.e.*, the λ_{Y^*}-oscillator) can become excited. This drastically reduces the number of states that must be summed over. Unfortunately, this simplification does not apply for $u\bar{u}$ or $d\bar{d}$ pair creation.

It is useful to refer to the closure-spectator limit of Eq. (2). This is the limit in which the energy denominators do not depend strongly on the quantum numbers of Y^* and K^*, so that the sums over intermediate states collapse to 1, giving

$$\langle O_s \rangle \propto \langle p \,| h_{s\bar{s}} O_s h_{s\bar{s}} |\, p \rangle \propto \langle 0 \,| h_{s\bar{s}} O_s h_{s\bar{s}} |\, 0 \rangle \ , \tag{4}$$

where the second step follows since $h_{s\bar{s}}$ does not couple to the motion of the valence spectator quarks. We see that the expectation value of O_s is taken between the $^3P_0$ states created by $h_{s\bar{s}}$. From the J^{PC} of the $^3P_0$ pair it then follows that $\Delta s = R_s^2 = \mu_s = 0$ in the closure-spectator limit (a result which

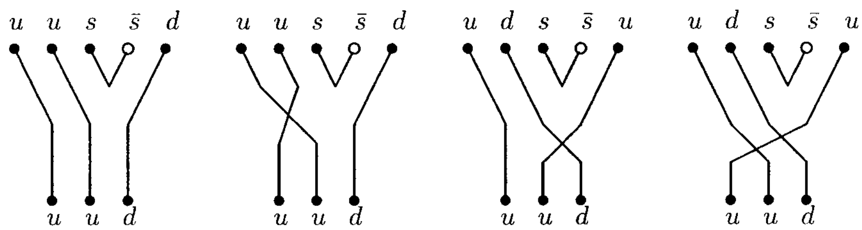

Figure 6: Quark line diagrams for $p \rightarrow \Sigma^* K^*$ and $p \rightarrow \Lambda^* K^*$.

would not be seen if only the lowest term, or lowest few terms, were included in the closure sum).

In the next Section I will discuss the results for the expectation values defined by Eq. (2) for the quantities Δs, R_s^2, and μ_s. We will see that delicate cancellations lead to small values for these observables even though the probability of $s\bar{s}$ pairs in the proton is substantial.

4.1 Strange Spin Content

Δs, the fraction of the proton's spin carried by strange quarks, is given by twice the expectation value of the s and $\bar{s}$ spins :

$$\Delta s = 2 \left\langle S_z^{(s)} + S_z^{(\bar{s})} \right\rangle . \tag{5}$$

Let us first examine the contribution to Δs from just the lowest-lying intermediate state, ΛK. The P-wave ΛK state with $J = J_z = \frac{1}{2}$ is

$$\left|(\Lambda K)_{P\frac{1}{2}}\right\rangle = \sqrt{\frac{2}{3}}\left|(\Lambda_\downarrow K)_{m=1}\right\rangle - \sqrt{\frac{1}{3}}\left|(\Lambda_\uparrow K)_{m=0}\right\rangle . \tag{6}$$

The $\bar{s}$ quark in the kaon is unpolarized, while the s quark in the Λ carries all of the Λ's spin; because of the larger coefficient multiplying the first term in (6), the ΛK intermediate state alone gives a negative contribution to Δs.

When we add in the $(\Lambda K^*)_{P\frac{1}{2}}$ and $(\Lambda K^*)_{P\frac{3}{2}}$ states (note that the subscripts denote the quantities ℓS defined previously), we have

$$\Delta s \propto \begin{pmatrix} 1 & -\sqrt{\frac{1}{3}} & \sqrt{\frac{8}{3}} \end{pmatrix} \frac{1}{18} \begin{bmatrix} -3 & \sqrt{3} & -\sqrt{24} \\ & -1 & \sqrt{8} \\ & & 10 \end{bmatrix} \begin{pmatrix} 1 \\ -\sqrt{\frac{1}{3}} \\ \sqrt{\frac{8}{3}} \end{pmatrix} \tag{7}$$

in the closure limit. Here the matrix is just $2(S_z^{(s)} + S_z^{(\bar{s})})$ (which is of course symmetric), and the vectors give the relative coupling strengths of the proton to $[\ (\Lambda K)_{P\frac{1}{2}},\ (\Lambda K^*)_{P\frac{1}{2}},\ (\Lambda K^*)_{P\frac{3}{2}}\ ]$. There are a couple of things to note here:

(1) The matrix multiplication in (7) evaluates to zero; there is no net contribution to Δs from the ΛK and ΛK^* states in the closure limit. There are in fact many such "sub-cancellations" in the closure sum for Δs: for each fixed set of spatial quantum numbers in the intermediate state, the sum over quark spins alone gives zero (because $\langle S_z^{(s)}\rangle = \langle S_z^{(\bar{s})}\rangle = 0$ in the $^3P_0$ state). That is, each $SU(6)$ multiplet inserted into Eq. (2) separately sums to zero. Moreover, the Δs operator does not cause transitions between $I = 0$ and $I = 1$ strange baryons so that the Λ and Σ sectors are decoupled, hence they individually sum to zero.

(2) Only the diagonal term in Eq. (7) corresponding to $p \to (\Lambda K^*)_{P\frac{3}{2}} \stackrel{\Delta s}{\to} (\Lambda K^*)_{P\frac{3}{2}} \to p$ gives a positive contribution to Δs. (Here $\stackrel{\Delta s}{\to}$ denotes the action of the Δs operator.) All of the other terms give negative contributions. In the full calculation with energy denominators, the negative terms are enhanced because they contain kaon (rather than K^*) masses. The full calculation gives $\Delta s = -0.065$ from ΛK and ΛK^* states. The largest individual contribution is -0.086, from the off-diagonal term $p \to (\Lambda K)_{P\frac{1}{2}} \stackrel{\Delta s}{\to} (\Lambda K^*)_{P\frac{3}{2}} \to p$.

For intermediate states containing Σ and Σ^* baryons, one finds as expected a net Δs from these states of zero in the closure limit, but this time the insertion of energy denominators does not spoil the cancellation very much: the full calculation gives $\Delta s = -0.003$ in this sector.

P-wave hyperons and kaons contribute another -0.04 to Δs, and the net contribution from all higher states is -0.025. *Thus, the result of the calculation*[10] *is* $\Delta s = -0.13$, in quite good agreement with the most recent extractions from experiment. It should be emphasized that all parameters of this calculation were fixed by spectra and decay data. Moreover, the result is quite stable to parameter changes.

For comparison with other calculations, note that the ΛK intermediate state alone contributes -0.030 to Δs, and the contribution from the ΛK, ΣK, and $\Sigma^* K$ states together is (coincidentally) also -0.030.

4.2 Note on the Spin Crisis

With this background in mind, let me make some comments on the spin crisis. In the spirit of "valence quark plus glue with $q\bar{q}$ corrections", let us write

$$\Delta q = \Delta q_{valence} + \Delta q_{sea}$$

and note that:

1. Given the earlier discussion, we do not expect the nonrelativistic result $\Delta q_{valence} = 1$ since the lower components of the relativistic valence quarks developed *via* Z-graphs typically reduce their contributions to $\Delta q_{valence} \simeq 0.75$.

2. Since $\Delta q_{sea} = \sum_f \Delta q_{sea}^{(f)}$, where $\Delta q_{sea}^{(f)}$ is the spin sum contribution of the quark-antiquark sea of flavor f, if there are N_f approximately flavor-symmetric light quark flavors then $\Delta q_{sea} \simeq N_f \Delta q_{sea}^{(f_1)}$, where f_1 is the first of these light flavors. Note that no matter how suppressed $\Delta q_{sea}^{(f_1)}$ might be, if $N_f >> N_c$, $\Delta q - \Delta q_{valence}$ will be large. In other words, although the spin crisis makes the valence approximation look bad, what is relevant for the approximation is that $\Delta q_{sea}^{(s)} << \Delta q_{valence}$ which is indeed what is observed experimentally.

3. A possible scenario for the spin crisis is that $\Delta q_{valence} \simeq 0.75$, $\Delta q_{sea}^{(s)} \simeq -0.13$, $\Delta q_{sea}^{(u)} \simeq -0.16$, and $\Delta q_{sea}^{(d)} \simeq -0.16$ (where we have speculatively included a small $SU(3)$-breaking effect) leading to $\Delta q \simeq 0.3$. If this scenario is correct, then the spin crisis will have shown us [16] that the valence quarks behave just as they were supposed to do!

We can expect that, within the intrinsic systematic errors, Δu, Δd,and Δs will be known in another year or two. Then, the next logical step will be to determine the contribution of sea quarks, and the strange quarks in particular, to the static properties of the nucleons. Using parity violation as a probe, the SAMPLE experiment at MIT's Bates Lab and an extensive program of measurements planned for CEBAF at Jefferson Lab (including measurements utilizing the existing Hall A spectrometers as well as a new special purpose detector called G^0 funded for construction in Hall C) will allow us to decompose the nucleon form factors into their quark-level components: G_E^u, G_E^d, G_E^s, and G_M^u, G_M^d, G_M^s each as a function of Q^2. Predictions relevant to these measurements are described in the next two subsections.

4.3 Strangeness Radius

The calculation of R_s^2 is more difficult than the calculation of Δs, for several reasons. First, the operators appearing in R_s^2 cause orbital and radial transitions among the intermediate states. Thus SHO transitions satisfying $\Delta n = 0, \pm 1$ and/or $\Delta \ell = 0, \pm 1$ are allowed, so there are many more terms to calculate (n and ℓ are orbital and radial SHO quantum numbers). Moreover,

Table 1: Proton strangeness radius from hadronic loops (in fm^2). The rows give the running totals as progressively more excited intermediate states are added into the calculation. The final column shows the total from all intermediate states.

	S-waves	plus P-waves	plus D-waves and S-wave radial excitations	all states
r_s^2	.097	.198	.210	.173
$r_{\bar{s}}^2$	.094	.139	.185	.210
R_s^2	.003	.059	.025	−.04

the sub-cancellations discussed above no longer occur, so that R_s^2 converges more slowly than Δs: more states must be included in Eq.(2) to obtain good accuracy. In addition, the basic matrix elements are more complicated.

The results for R_s^2 are shown in Table 1. With the standard parameter set, $R_s^2 = -0.04\mathrm{fm}^2$. For reasonable parameter variations, R_s^2 ranges between -0.02 and $-0.06\mathrm{fm}^2$. Table 1 shows that the lowest-lying $SU(6)$ multiplets of intermediate states (*i.e.*, the S-wave hyperons and kaons) account for about half of r_s^2 and $r_{\bar{s}}^2$. Most of the remaining contributions come from P-wave hyperons and kaons. However, R_s^2 involves a large cancellation between r_s^2 and $r_{\bar{s}}^2$, and its value doesn't settle down until we add in quite highly excited intermediate states. For this reason, the precise numerical value (and perhaps even the sign) of R_s^2 cannot be considered definitive: the conclusion is rather that R_s^2 is small, about an order of magnitude smaller than r_s^2 and $r_{\bar{s}}^2$. This result is not too surprising: R_s^2 is exactly zero in the closure limit, and previous hadronic loop studies[8,9] led one to expect that the full calculation with energy denominators would preserve the qualitative features of this limit.

Note that the ΛK intermediate state alone gives $R_s^2 \approx -0.01\mathrm{fm}^2$ (the sign is as expected from the usual folklore) while the ΛK, ΣK, and $\Sigma^* K$ states together give $-0.017\mathrm{fm}^2$. Nevertheless, although the sum over all states gives the same sign and order of magnitude as these truncations, Table 1 shows that this is just a coincidence.

4.4 Strange Magnetic Moment

The strange and antistrange quarks carry magnetic moments $-\frac{1}{3}\mu^{(s,\bar{s})}$ where

$$\mu^{(s)} = \frac{1}{2m_s}\langle 2S_z^{(s)} + L_z^{(s)}\rangle \tag{8}$$

$$\mu^{(\bar{s})} = -\frac{1}{2m_s}\langle 2S_z^{(\bar{s})} + L_z^{(\bar{s})}\rangle \tag{9}$$

Table 2: Proton strangeness magnetic moment from hadronic loops

	$\langle 2S_z \rangle$	$\langle L_z \rangle$	μ_s (in nuclear magnetons μ_N)
s quarks	-0.058	+0.043	-0.025
$\bar{s}$ antiquarks	-0.074	+.038	+0.060
total			+0.035

and we denote the net strange magnetic moment by μ_s:

$$\mu_s \equiv \mu^{(s)} + \mu^{(\bar{s})}. \tag{10}$$

Computing the expectation values of these operators presents no new difficulties beyond those encountered in the R_s^2 calculation. In fact, there are no radial transitions in this case, so there are fewer states to sum over and the sum converges more quickly.

The result (see Table 2) is a positive (albeit small) value for μ_s, in disagreement with most other models. Where does the positive sign originate? First note that the signs of $\langle S_z^{(s)} \rangle$, $\langle L_z^{(s)} \rangle$, and $\langle L_z^{(\bar{s})} \rangle$ are correctly given by just the lowest lying intermediate state, ΛK of Eq. (6). (Note that the L_z's have similar magnitudes so that orbital angular momentum contributes very little to μ_s in any case.) On the other hand, the ΛK state has $\langle S_z^{(\bar{s})} \rangle = 0$, whereas $\langle S_z^{(\bar{s})} \rangle$ is quite large and negative. (The main contribution comes from the off-diagonal process $p \to (\Lambda K)_{P\frac{1}{2}} \xrightarrow{S_z^{(\bar{s})}} (\Lambda K^*)_{P\frac{3}{2}} \to p$, although there is also a significant contribution from $p \to (\Lambda(1405)K)_{S\frac{1}{2}} \xrightarrow{S_z^{(\bar{s})}} (\Lambda(1405)K^*)_{S\frac{1}{2}} \to p$.) These important terms, which drive μ_s positive, are omitted in calculations which include only kaon loops. (The ΛK intermediate state alone contributes $-0.080\mu_N$ to μ_s, and the contribution from ΛK, ΣK, and $\Sigma^* K$ together is $-0.074\mu_N$.)

5 Summary

In these lectures I have advocated treating the phenomenology of QCD in two steps. In the zeroth order, strong QCD is approximated by a relativistic constituent quark model with flux tube gluodynamics. As a second step, $q\bar{q}$ sea and other $1/N_c$ effects are added as perturbations.

We have seen here how the quark model might be "unquenched" in a way that preserves its spectroscopic successes and respects the OZI rule. All of the results presented are qualitative, but the picture appears to offer a viable explanation of the underlying physics. The key asumptions of the model are that flux tube dyanamics, including a flux tube full of $q\bar{q}$ pairs, can be treated adiabatically, and that the $q\bar{q}$ pair creation occurs into a state with vacuum quantum numbers ($^3P_0$ or $J^{PC} = 0^{++}$).

The main new results of the picture I have advocated are:

1. The quark model spectrum is immune to meson-loop-induced mass shifts apart from those associated with nearby thresholds. By systematically incorporating the adiabatic effects into the definition of the quark model potential, a systematic low energy expansion of the effects of thresholds is possible [11].

2. The OZI rule survives loops corrections, once they are done systematically; an exception to this rule will occur for $J^{PC} = 0^{++}$ mesons since their mixing is not zero in the closure limit [9].

3. Both of the preceeding results are associated with insights into the extent of the set of hadronic states required to respect the dualities which underlie them, and they strongly suggest that low energy hadronizations of QCD are in trouble, since sums over large towers of states were required.

4. $\Delta s \simeq -0.13$, which when combined with comparably polarized u and d sea quarks and with $\Sigma_{valence} \sim 0.75$, suggests [16] that the valence quarks are actually "normal", with the sea quarks responsible for the spin crisis.

5. μ_s and ${r^2}_s$ are small.

The physical picture underlying these results also suggests that one may expect that:

1. Sea effects will generally be small in static current matrix elements.

2. An exception to this rule will occur for $J^{PC} = 0^{++}$ currents since they are not zero in the closure limit.

3. To the extent that the adiabatic approximation holds, sea quark effects will play minor rôles in hadronic form factors (and in particular charge radii) [17].

4. Associated with the suppression of $q\bar{q}$ effects in charge radii will be an associated resonance dominance of nonsinglet-current-induced processes, since nonresonant contributions will be associated with the failure of the adiabatic approximation [17].

Sea quark effects, most easily studied *via* the $s\bar{s}$ content of the proton, thus could open a window on some of the key issues in strong QCD: the applicability of the adiabatic limit, the origin of the effective quark model potential, the nature of the OZI rule, and the mechanisms behind quark-hadron duality. The precision determination of the properties of this sea are thus of the utmost importance.

References

1. F.E. Close, private communication, cogently advocates using the positive term "strong QCD" instead of the negative "nonperturbative QCD".
2. G. 't Hooft, Nucl. Phys. **B72**, 461 (1974); E. Witten, Nucl. Phys. **B160**, 57 (1979).
3. S. Okubo, Phys. Lett. **5**, 165 (1963); Phys. Rev. D **16**, 2336 (1977); G. Zweig, CERN Report No. 8419 TH 412, 1964 (unpublished); reprinted in *Developments in the Quark Theory of Hadrons*, edited by D. B. Lichtenberg and S. P. Rosen (Hadronic Press, Massachusetts, 1980); J. Iizuka, K. Okada, and O. Shito, Prog. Th. Phys. **35**, 1061 (1966); J. Iizuka, Prog. Th. Phys. Suppl. **37-38**, 21 (1966).
4. N. Isgur and M.B. Wise, Phys. Lett. **B237**, 527 (1990); **B232**, 113 (1989); Phys. Rev. Lett. **66**, 1130 (1991); and in *B Decays*, ed. S. Stone (World Scientific, Singapore, 1991), p. 158.
5. N. Isgur and J. Paton, Phys. Rev. D **31**, 2910 (1985).
6. For a review of the adiabatic approximation in the context of the flux tube model see N. Isgur in Proceedings of *Few Body Problems in Physics*, AIP Conf. Proc. **334**, ed. F. Gross (A.I.P., New York, 1995), p. 3. The proof that V has this general expansion for heavy quarks may be found in E. Eichten and F. Feinberg, Phys. Rev. D**23**, 2724 (1981).
7. See, e.g., S. Perantonis and C. Michaels, Nucl. Phys. **B347**, 854 (1990).
8. P. Geiger and N. Isgur, Phys. Rev. D **41**, 1595 (1990).
9. P. Geiger and N. Isgur, Phys. Rev. D **44**, 799 (1991); Phys. Rev. Lett. **67**, 1066 (1991); Phys. Rev. D **47**, 5050 (1993); P. Geiger, *ibid.* **49**, 6003 (1993).
10. P. Geiger and N. Isgur, Phys. Rev. D **55**, 229 (1997).
11. See, for example, N. Isgur, "Beyond the Adiabatic Approximation: the impact of thresholds on the hadronic spectrum", JLAB-THY-99-01.
12. H.J. Lipkin, Nucl. Phys. **B291**, 720 (1987); Phys. Lett. **B179**, 278 (1986); Nucl. Phys. **B244**, 147 (1984); Phys. Lett. **B124**, 509 (1983).
13. L. Micu, Nucl. Phys. **B10**, 521 (1969); A. Le Yaouanc, L. Oliver, O. Pene, and J.-C. Raynal, Phys. Rev. D **8**, 2233 (1973); Phys. Lett. **B71**,

397 (1977); *ibid.* **B72** , 57 (1977); W. Roberts and B. Silvestre-Brac, Few Body Syst. **11**, 171 (1992); P. Geiger and E.S. Swanson, Phys. Rev. D **50**, 6855 (1994).
14. R. Kokoski and N. Isgur, Phys. Rev. D **35**, 907 (1987);
15. Fl. Stancu and P. Stassart, Phys. Rev. D **38**, 233 (1988); **39**, 343 (1989); **41**, 916 (1990); **42**, 1521 (1990); S. Capstick and W. Roberts, Phys. Rev. D **47**, 1994, (1993); Phys. Rev. D **49**, 4570, (1994).
16. N. Isgur, "Valence Quark Spin Distribution Functions", JLAB-THY-98-23, hep-ph/9809255, to appear in Phys. Rev. **D**.
17. See, for example, N. Isgur, "Nonresonant States in Semileptonic Heavy Quark Decay: their structure, strength, and significance", in preparation.